Inorganic Chemistry

Article

pubs.acs.org/IC

Carbon Dioxide Promoted H^+ Reduction Using a Bis(imino)pyridine Manganese Electrocatalyst

Tufan K. Mukhopadhyay,[†] Nicholas L. MacLean,[†] Lu Gan,[†] Daniel C. Ashley,[‡] Thomas L. Groy,[†] Mu-Hyun Baik,*[,‡] Anne K. Jones,*[,†] and Ryan J. Trovitch*[,†]

[†]Department of Chemistry & Biochemistry, Arizona State University, Tempe, Arizona 85287, United States

[‡]Department of Chemistry, Indiana University, Bloomington, Indiana 47405, United States

Supporting Information

ABSTRACT: Heating a 1:1 mixture of $(CO)_5MnBr$ and the phosphine-substituted pyridine diimine ligand, ^{Ph2PPr}PDI, in THF at 65 °C for 24 h afforded the diamagnetic complex [(^{Ph2PPr}PDI)-Mn(CO)][Br] (**1**). Higher temperatures and longer reaction times resulted in bromide displacement of the remaining carbonyl ligand and the formation of paramagnetic (^{Ph2PPr}PDI)MnBr (**2**). The molecular structure of **1** was determined by single crystal X-ray diffraction, and density functional theory (DFT) calculations indicate that this complex is best described as low-spin Mn(I) bound to a neutral ^{Ph2PPr}PDI chelating ligand. The redox properties of **1** and **2** were investigated by cyclic voltammetry (CV), and each complex was tested for electrocatalytic activity in the presence of both CO_2 and Brønsted acids. Although electrocatalytic response was not observed when CO_2, H_2O, or MeOH was added to **1** individually, the addition of H_2O or MeOH to CO_2-saturated acetonitrile solutions of **1** afforded voltammetric responses featuring increased current density as a function of proton source concentration (i_{cat}/i_p up to 2.4 for H_2O or 4.2 for MeOH at scan rates of 0.1 V/s). Bulk electrolysis using 5 mM **1** and 1.05 M MeOH in acetonitrile at −2.2 V vs $Fc^{+/0}$ over the course of 47 min gave H_2 as the only detectable product with a Faradaic efficiency of 96.7%. Electrochemical experiments indicate that CO_2 promotes **1**-mediated H_2 production by lowering apparent pH. While evaluating **2** for electrocatalytic activity, this complex was found to decompose rapidly in the presence of acid. Although modest H^+ reduction activity was realized, the experiments described herein indicate that care must be taken when evaluating Mn complexes for electrocatalytic CO_2 reduction.

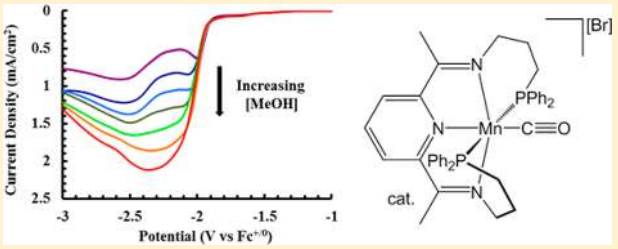

INTRODUCTION

Storing solar energy by using it to convert abundant low-energy molecules into high-energy commodity chemicals that may be used as fuel is a critical future technology.[1,2] A key component of such technology is a reduction catalyst that acts in concert with an oxidation catalyst and a light harvesting device to efficiently drive an uphill reaction. To be economically viable and deployable on a large scale, the catalyst material should only use inexpensive and highly abundant elements.[3] Recent efforts have produced a number of interesting first-row metal complexes[4−6] capable of reducing, for example, H^+ to hydrogen gas.[7] Whereas hydrogen gas could be used directly as a fuel, the inconveniences of storage and transport[8] render CO_2 reduction products much more interesting targets.[9] The electrocatalytic reduction of carbon dioxide may give a variety of products,[10] of which carbon monoxide and formic acid are most frequently encountered.

Recently, several remarkable CO_2 reduction catalysts based on first-row metals have been reported.[11−13] Chardon-Noblat and Deronzier[14] showed that Mn complexes of the general formula (bpy-R_2)$(CO)_3$MnX (bpy-R_2 = 4,4′-disubstituted-2,2′-bipyridine, X = halide) can convert CO_2 to CO electrocatalytically with selectivities that are comparable to their widely investigated Re congeners.[15] Subsequently, Kubiak demonstrated that (bpy-^{t}Bu$_2$)$(CO)_3$MnBr catalyzes the reduction of CO_2 to CO with a turnover frequency (TOF) of 340 s^{-1} at −2.2 V vs SCE in the presence of 1 M 2,2,2-trifluoroethanol.[16] The 6,6′-dimesityl-substituted bpy ligand is thought to prevent catalyst dimerization, increasing the TOF of CO_2 reduction to 5,000 s^{-1}.[17] When employed with a Ru(II) photosensitizer, (bpy)$(CO)_3$MnBr was shown to convert CO_2 to formic acid with a turnover number (TON) of 149, while producing minor amounts of CO and H_2 with TONs of 12 and 14, respectively.[18] When cast in a Nafion film on a glassy carbon electrode, (bpy)$(CO)_3$MnBr mediated CO_2 reduction resulted in the simultaneous formation of CO and H_2 approximately in a ratio of 1:2.[19] Being thermodynamically preferred, the coproduction of H_2 is often observed during electrocatalytic CO_2 reduction, and dedicated Mn-based H^+ reduction catalysts have been reported.[20]

Many Mn-complexes capable of reducing CO_2 carry bpy ligands,[21] but some α-diimine[22] and 2-pyridyl-*N*-heterocyclic carbene[23] complexes of Mn have also been reported to be catalytically active. Redox noninnocence of the bpy[24] and α-diimine[25] ligands is believed to be key to CO_2 reduction. By

Received: February 9, 2015
Published: April 22, 2015

DOI: 10.1021/acs.inorgchem.5b00315
Inorg. Chem. 2015, 54, 4475−4482

storing electrons not only on the metal but also on the ligands during the formation of the catalytically competent intermediates,[15d,22b] these complexes are thought to access formal oxidation states that are unusually low with relatively small energetic penalties. Thus, we hypothesized by analogy that redox noninnocent 2,6-bis(imino)pyridine (or pyridine diimine, PDI) ligands[26] may form electrocatalytically active complexes, as indicated in Figure 1. Having previously

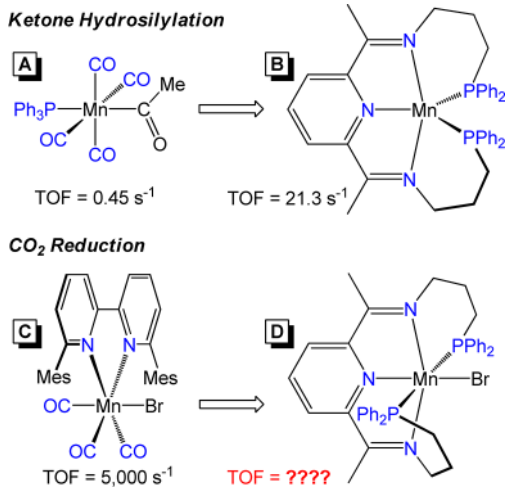

Figure 1. Considering a pentadentate PDI chelate for Mn-based electrocatalytic CO_2 reduction. Formally neutral ligands are shown in blue. By analogy, we speculate that **D** may be an active CO_2 reduction catalyst, as indicated by the question marks for TOF in red.

discovered that (κ^5-*N,N,N,P,P*-^{Ph2PPr}PDI)Mn[27] exhibits carbonyl hydrosilylation activities that are 45 times greater than those reported for $(Ph_3P)(CO)_4MnC(O)CH_3$ (Figure 1, **B** and **A**, respectively),[28,29] herein we describe a series of (PDI)Mn complexes that mimic the $(bpy)(CO)_3MnBr$ system (Figure 1) but prevent the unproductive catalyst dimerization side reaction observed for the prominent $(bpy)(CO)_3MnBr$ catalyst.[14]

RESULTS AND DISCUSSION

Synthesis and Characterization. A stoichiometric quantity of the ^{Ph2PPr}PDI ligand[30] was added to a THF solution of $(CO)_5MnBr$ (eq 1). Although no immediate change was

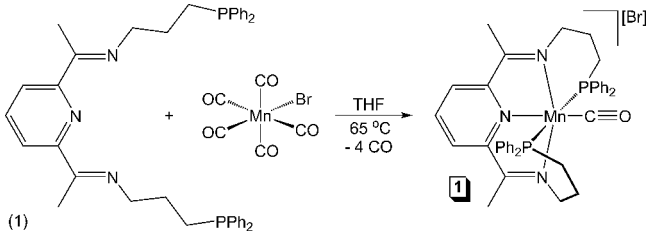

observed at ambient temperature, heating the reaction in a thick-walled glass vessel to 65 °C for 24 h resulted in a dark solution and a significant amount of purple precipitate. Isolation of the precipitate and analysis by ^{31}P NMR spectroscopy revealed a single resonance at 55.42 ppm, suggesting that the chelating phosphine substituents are equivalent and attached to Mn. Infrared spectroscopy revealed a single CO stretch at 1825 cm^{-1}, identifying this product as the monocarbonyl complex, [(^{Ph2PPr}PDI)Mn(CO)][Br] (eq 1, **1**). This formulation is further supported by the poor solubility of **1** in nonpolar solvents.

The composition of **1** was confirmed by single crystal X-ray diffraction (Figure 2), and the metrical parameters determined

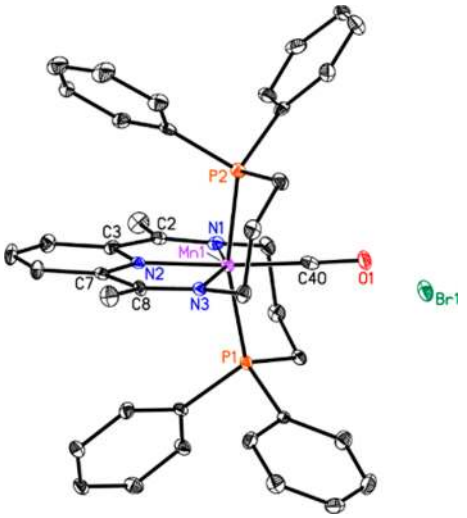

Figure 2. Solid state structure of **1** shown at 30% probability ellipsoids. Hydrogen atoms and a cocrystallized pentane molecule are omitted for clarity.

Table 1. Experimental Bond Lengths (Å) and Angles (deg) Determined for 1

	1
Mn(1)−N(1)	1.981(5)
Mn(1)−N(2)	1.931(4)
Mn(1)−N(3)	1.996(5)
Mn(1)−P(1)	2.2777(17)
Mn(1)−P(2)	2.2974(18)
Mn(1)−C(40)	1.773(7)
C(40)−O(1)	1.177(7)
N(1)−C(2)	1.311(7)
N(3)−C(8)	1.310(8)
C(2)−C(3)	1.456(8)
C(7)−C(8)	1.446(8)
N(2)−C(3)	1.354(6)
N(2)−C(7)	1.370(7)
N(1)−Mn(1)−N(3)	155.14(19)
P(1)−Mn(1)−P(2)	162.95(7)
N(2)−Mn(1)−C(40)	176.2(2)
Mn(1)−C(40)−O(1)	178.0(5)

for this complex are provided in Table 1. The geometry about the Mn center of **1** can best be described as distorted octahedral with N(1)−Mn(1)−N(3) and P(1)−Mn(1)−P(2) angles of 155.14(19) and 162.95(7)°, respectively. The Mn−N [1.981(5), 1.931(4), and 1.996(5) Å] and Mn−P [2.2777(17) and 2.2974(18) Å] distances are relatively short, indicative of a low-spin Mn electronic configuration.[27,31] Importantly, inspection of the PDI chelate imine C═N distances reveals moderate elongation [1.311(7) and 1.310(8) Å] relative to those determined for unreduced PDI ligands (1.28 Å).[26b] The C(2)−C(3) and C(7)−C(8) distances determined for **1** of 1.456(8) and 1.446(8) Å, respectively, are significantly

DOI: 10.1021/acs.inorgchem.5b00315
Inorg. Chem. 2015, 54, 4475−4482

contracted from the $C_{imine}-C_{pyridine}$ distances found for unreduced chelates (1.50 Å).[26b] Taken together, these parameters suggest that **1** might possess a PDI chelate monoanion that is antiferromagnetically coupled to a low-spin Mn(II) center.

To further clarify the electronic structure, density functional theory (DFT) calculations were performed on **1**. Ongoing unpublished work in our laboratory on (κ^5-*N,N,N,P,P*-^{Ph2PPr}PDI)Mn (Figure 1, **B**) showed that the PBE functional provided good agreement with the experimental crystal structure and ground spin state. Therefore, we started by employing this method. Our calculations confirmed that **1** is a ground-state singlet, with the triplet state lying 17.3 kcal/mol higher in energy. This singlet converged to a closed-shell state that is well-formulated as a Mn(I) state as shown in the qualitative molecular orbital diagram in Figure 3. The triplet

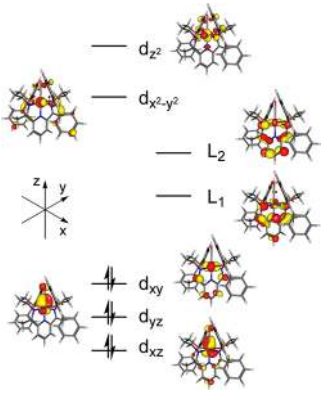

Figure 3. Energy-level diagram illustrating the calculated frontier orbitals of **1**.

involved promotion of an electron from the d_{xy} orbital into one of the PDI-based ligand orbitals (L1). A broken-symmetry orbital solution could be found for the triplet geometry, but attempts to perform a geometry optimization resulted in collapse to the closed-shell state. It is a reasonable assumption that the triplet and broken-symmetry singlet have similar geometries if the coupling between the electrons is weak; so, we evaluated the energy of the broken-symmetry singlet at this geometry. As is typically the case, the broken-symmetry singlet was essentially isoenergetic with the triplet. This relative stability of the closed-shell configuration is likely due to the stabilizing effect of the π-acidic CO ligand, which lowers the energy of the metal-based (pseudo)-t_{2g} orbitals by removing electron density from the metal center and therefore increasing the energetic penalty for exciting an electron into a PDI-based orbital.

As pure-GGA functionals such as PBE have a tendency to overestimate the stability of low-spin states, we decided to perform single-point energy evaluations on our PBE geometries using the hybrid functional B3LYP to see if spin-state ordering would be significantly functional dependent. Using B3LYP, the triplet state is 8.2 kcal/mol higher in energy than the closed-shell singlet. The broken-symmetry singlet is still effectively isoenergetic with the triplet. Despite the large change in the magnitude of the spin-state energetics, the closed-shell singlet is still predicted to be lower in energy than spin-states that invoke a reduced PDI-ligand.

While the optimized structures of both the triplet and singlet states for **1** agree reasonably well with the crystallographic bond lengths for the PDI ligand, the Mn−P bond lengths show significant differences for the two spin states. The Mn−P bond lengths are significantly longer than the crystal structure for the triplet (both are 2.41 Å), whereas the singlet Mn−P bond lengths are a closer match (both are 2.34 Å). As mentioned earlier, it is likely that the broken-symmetry singlet geometry is very similar to the triplet, and hence, this structural difference further confirms the assignment of the ground state as a closed shell singlet (Figure 3). These computational results suggest that **1** possesses an unreduced PDI chelate and that crystallographically observed $N_{imine}-C_{imine}$ bond elongation and $C_{imine}-C_{pyridine}$ bond contraction are due to Mn-to-PDI backbonding rather than one-electron reduction of the chelate.

During preparations of **1**, small quantities of a bright blue, toluene-soluble product were collected from reactions allowed to stir at 65 °C for longer than 24 h. To characterize this side product, an equimolar mixture of ^{Ph2PPr}PDI and $(CO)_5$MnBr in THF was intentionally heated to 80 °C for 72 h. The removal of CO and solvent allowed for the isolation of a bright blue, paramagnetic solid which has been identified as (^{Ph2PPr}PDI)-MnBr (eq 2, **2**). When analyzed by infrared spectroscopy,

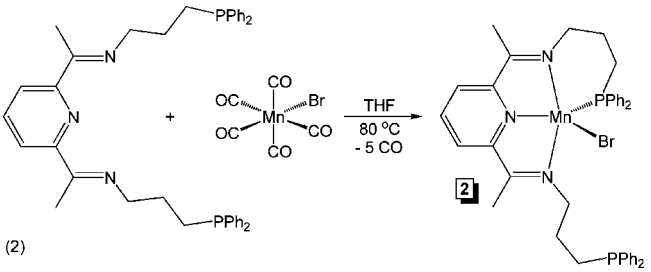

stretching frequencies consistent with CO coordination are absent, suggesting that complete carbonyl ligand displacement occurs. The ^{1}H NMR spectrum exhibits a predominant paramagnetically shifted resonance at 74.68 ppm, while signals attributable to **2** were not observed by ^{13}C NMR spectroscopy. The magnetic susceptibility of this complex is 4.4 μ_B at 297 K (Evans method), suggesting a high spin Mn(II) center that is antiferromagnetically coupled to a κ^4-*N,N,N,P*-^{Ph2PPr}PDI radical monoanion. Complex **2** has also been prepared by heating samples of **1** under vacuum.

Electrochemistry. The redox properties of **1** and **2** were analyzed by cyclic voltammetry. In 0.1 M $[Bu_4N][PF_6]$ acetonitrile solution, cyclic voltammograms of **1** were found to feature two reversible waves with midpoint potentials of −0.30 V and −1.92 vs $Fc^{+/0}$ (all potentials are quoted relative to $Fc^{+/0}$ as an internal standard; Figure 4). The smaller wave at −0.30 V is attributed to the one electron oxidation of **1** to form the Mn(II) complex, whereas the two-electron reduction wave at −1.92 V is associated with the formation of the formally Mn(-I) complex, which is likely to possess a reduced PDI chelate, such that (PDI^-)Mn(0) is a more appropriate representation of the electronic structure. Bulk electrolysis experiments revealed that the wave at −1.92 V becomes irreversible after passing more than 2.0 F/mol of charge, supporting the assignment of a two-electron reduction (Figure S7, Supporting Information). The observation of a two-electron reduction, instead of a pair of successive one-electron reductions suggests that **1** does not dimerize upon reduction, as has been reported for (bpy-^{t}Bu$_2$)$(CO)_3$MnBr.[16] Although reduction of **1** occurs at a potential 370 mV more negative than the reversible two-electron reduction reported for (bpy-

DOI: 10.1021/acs.inorgchem.5b00315
Inorg. Chem. 2015, 54, 4475−4482

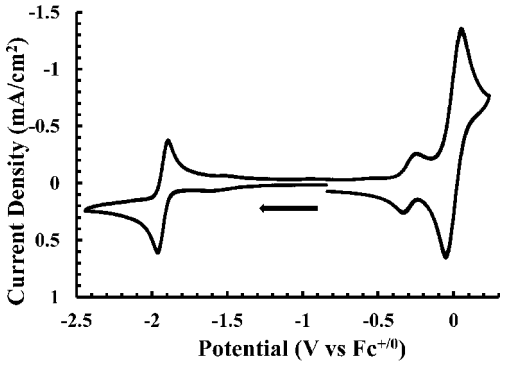

Figure 4. Cyclic voltammogram of **1** in 0.1 M $[Bu_4N][PF_6]$ acetonitrile. Ferrocene used as an internal standard (wave centered at 0.0 V). Potential scan rate = 0.1 V s^{-1}. Arrow indicates the direction of cycling.

$Mes_2)(CO)_3MnBr$ (1.55 V),[17] the latter does not exhibit electrocatalytic CO_2 to CO reduction until approximately −2.0 V (overpotential = 0.7 V), rendering the redox properties of **1** promising for analogous activity. In contrast, cyclic voltammograms of **2** show only irreversible waves at −2.70 and −3.11 V, corresponding to complex reduction (Figure S8, Supporting Information).

To investigate the possibility that **1** is a CO_2 reduction precatalyst, cyclic voltammograms of this complex were collected in dry and wet CO_2-saturated acetonitrile.[32] As shown in Figure 5, the reduction at −2.03 V becomes

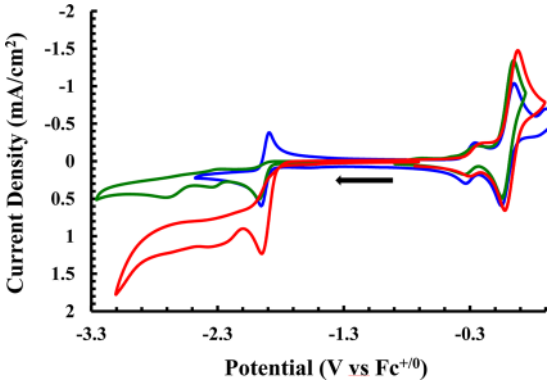

Figure 5. Cyclic voltammograms of **1** (blue), a solution of **1** saturated with CO_2 (green), and a CO_2-saturated solution of **1** containing 3.0 M H_2O (red). All voltammograms collected in 0.1 M $[Bu_4N][PF_6]$ acetonitrile using ferrocene as an internal standard (scan rate = 0.1 V s^{-1}). Complex **1** is present at 1 mM concentration in all three experiments. The arrow indicates the direction of cycling.

irreversible upon saturation of the solution with CO_2, but an increase in current was not detected. Data collected from a CO_2-saturated acetonitrile solution of **1** including 3.0 M H_2O showed a significant increase in current, indicating that **1** performs reductive catalysis in the presence of CO_2 and H_2O at approximately −1.9 V. Similar experiments were conducted using **2**, but H_2O addition resulted in immediate decomposition of the complex.

To characterize electrocatalysis by **1**, voltammograms were collected with varying quantities of Brønsted acid in CO_2-saturated 1 mM solutions of the complex. The current density in dry solvent at −1.98 V was 0.5 mA/cm^2; adding 3.15 M H_2O increased the current density to 1.2 mA/cm^2 (i_{cat}/i_p = 2.4, Figure 6A). Although this data is consistent with CO_2 reduction, the possibility that the catalysis is a result of

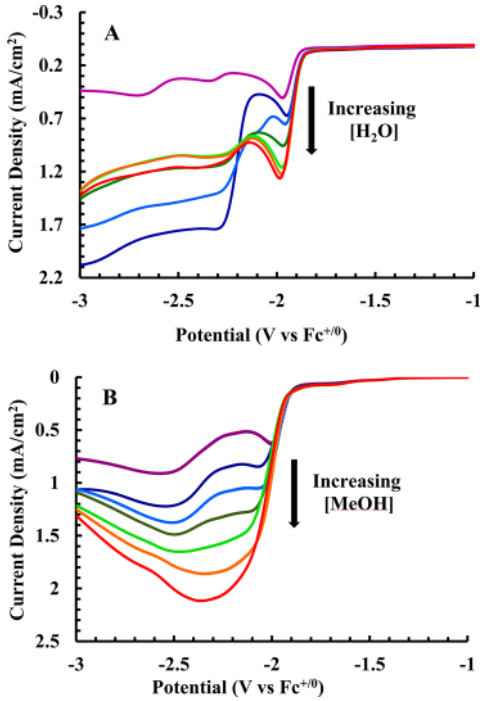

Figure 6. Partial cyclic voltammograms of **1** showing electrocatalytic reduction as a function of increasing H_2O (A) and methanol (B) concentration in CO_2-saturated 0.1 M $[Bu_4N][PF_6]$ acetonitrile. In A, no water (purple), 0.55 M H_2O (dark blue), 1.10 M H_2O (light blue), 1.65 M H_2O (dark green), 2.15 M H_2O (bright green), 2.65 M H_2O (orange), and 3.15 M H_2O (red). In B, 0.15 M MeOH (purple), 0.30 M MeOH (dark blue), 0.45 M MeOH (light blue), 0.60 M MeOH (dark green), 0.75 M MeOH (bright green), 0.90 M MeOH (orange), and 1.05 M MeOH (red). All voltammograms collected using ferrocene as an internal standard at a scan rate = 0.1 V s^{-1}. Complex **1** is present at 1 mM concentration in all experiments.

increased acidity was also considered by monitoring the apparent pH values of experimental solutions. The apparent pH of a dry, CO_2-saturated, acetonitrile solution is 9.3, but upon addition of 3.15 M H_2O that value drops to 7.7. To evaluate the impact of acidity on the observed electrocatalysis, nitrogen-saturated solutions of similar acidity and solvent composition to those in Figure 6A were created using an aqueous mixed pH buffer consisting of 15 mM each of MES, TAPS, HEPES, and CHES (see Experimental Procedures and Computational Details). Using these buffered solutions, comparable catalytic current was observed at −1.99 V without the addition of CO_2 (Figures S9 and S10, Supporting Information). This control experiment suggests the lowering of solution pH that results from the reaction of CO_2 with H_2O to form carbonic acid generates enough protons to promote **1**-mediated H_2 production. Since a number of first row transition metal complexes form nanoparticles on electrode surfaces, the "rinse test" was employed to ensure that the catalyst remains homogeneous. In short, the electrode was removed from a catalytically active solution containing 2.15 M H_2O in acetonitrile, rinsed with dry acetonitrile, and placed in a CO_2-saturated water/acetonitrile solution without catalyst. No activity was observed (Figure S11, Supporting Information),

DOI: 10.1021/acs.inorgchem.5b00315
Inorg. Chem. 2015, 54, 4475−4482

suggesting that electrode deposits and the electrode itself are not responsible for catalysis.

To avoid carbonic acid formation, analogous electrochemical experiments were conducted using anhydrous MeOH as an additive instead of H_2O. The addition of MeOH to CO_2-saturated 1 mM solutions of **1** results in current densities of up to 2.1 mA/cm^2 at −2.33 V (i_{cat}/i_p = 4.2 for 1.05 M MeOH, Figure 6B). Control experiments in nitrogen-saturated 1.1 M MeOH/acetonitrile were nearly identical to those in the absence of MeOH (0.8 vs 0.9 mA/cm^2 at −1.95 V, Figure 7). In

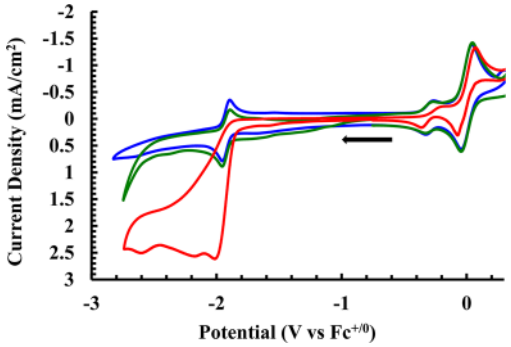

Figure 7. Cyclic voltammograms of **1** (blue), **1** in the presence of 1.1 M MeOH (no CO_2, green), and a CO_2-saturated solution of **1** containing 1.1 M MeOH (red). All voltammograms collected in 0.1 M $[Bu_4N][PF_6]$ acetonitrile solution using ferrocene as an internal standard (scan rate = 0.1 V s^{-1}). Complex **1** is present at 1 mM concentration in all three experiments. The arrow indicates the direction of potential cycling.

contrast, cyclic voltammograms obtained with 1.1 M MeOH in CO_2-saturated solutions afforded a current density of 2.6 mA/cm^2 (Figure 7), suggesting that CO_2 plays a role in the observed catalysis. Experiments conducted using catalyst-free, CO_2-saturated MeOH solutions showed no evidence for electrode-promoted H_2 production (Figure S12, Supporting Information). Since metal carbonyls are often light sensitive, voltammograms with 1.05 M MeOH were obtained in the dark, and a minimal decrease in catalytic current was noted (1.9 vs 2.1 mA/cm^2, Figure S13, Supporting Information).

Bulk electrolysis was conducted to determine the products formed during reductive catalysis by **1** in the presence of methanol. Notably, bulk electrolysis of a CO_2-saturated solution of 5 mM **1** and 1.05 M MeOH in acetonitrile at −2.2 V over 47 min produced H_2 as the sole product as determined by gas chromatography (there was no evidence for CO formation). Quantifying the H_2 produced as a function of time yielded a Faradaic efficiency of 96.7% and a modest TOF of 0.176 h^{-1} (Figure S14, Supporting Information). Analysis of the post-electrolysis solution by multinuclear NMR, infrared, and UV−visible spectroscopy (Figure S15, Supporting Information) demonstrated that **1** remained intact following electrolysis. This observation confirms that **1** does not scavenge newly generated CO and that the catalyst is stable beyond 47 min of active reduction.

Finally, the detection of H_2 following bulk electrolysis encouraged us to perform pH-controlled experiments in MeOH. The pseudo-pH of an acetonitrile solution containing 1 mM **1** and 1.05 M MeOH was found to be 9.8, and purging with a continuous flow of CO_2 resulted in a pseudo-pH value of 8.4. Separately, benzoic acid was added to an acetonitrile solution containing 1 mM **1** and 1.05 M MeOH to achieve a pseudo-pH of 8.1 in the absence of CO_2, and linear sweep voltammetry toward reducing potentials resulted in a current density of 1.5 mA/cm^2 at −1.96 V (Figure 8). While lower than

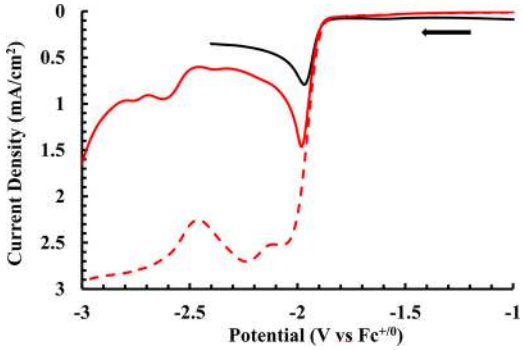

Figure 8. Linear sweep voltammograms of **1** (black), **1** in the presence of 1.05 M MeOH and 2 mM PhCOOH (solid red), and **1** in a CO_2-saturated acetonitrile solution containing 1.05 MeOH (dashed red). All voltammograms collected in 0.1 M $[Bu_4N][PF_6]$ acetonitrile solution using ferrocene as an internal standard (scan rate = 0.1 V s^{-1}). Complex **1** is present at 1 mM concentration in all three experiments. The arrow indicates the direction of potential cycling.

the peak current density observed under CO_2 (2.5 mA/cm^2, Figure 8), the voltammograms appear nearly identical over their comparable range (i.e., until di/dE = 0 for benzoic acid). The observation of catalytic current in the presence of benzoic acid is consistent with **1**-mediated H^+ reduction and is evidence that **1** does not reduce CO_2 throughout the course of H_2 production.

Taken together, the CV and bulk electrolysis experiments suggest that complex **1** is capable of producing H_2 from CO_2-acidified acetonitrile solutions of H_2O and MeOH. Although a six-coordinate inner-sphere bromide complex mimicking (bpy)-$(CO)_3$MnBr was initially targeted as an electrocatalyst (Figure 1, **D**), the inactivity of **2** in the presence of H_2O or MeOH suggests that the CO ligand of **1** is required for complex stabilization. Since carbonyl dissociation does not appear to occur during the course of catalysis (**1** is recovered following electrolysis), H^+ reduction is believed to take place following the reduction of **1** and concurrent dissociation of a ^{Ph2PPr}PDI phosphine group.[33] Although H_2 was not the desired electrolysis product, this study demonstrates that high-denticity chelates can prevent undesired electrocatalyst dimerization. Dimerization during Mn-catalyzed CO_2 reduction has recently been prevented with a 6,6′-dimesityl-substituted bpy ligand;[17] however, terdentate and tetradentate 2,2′-bypridine and α-diimine supporting chelates represent intriguing alternatives to incorporating steric bulk, as they offer an opportunity to simultaneously tune the electronic properties of the metal. More detailed mechanistic studies and additional work aiming at exploiting the relationship between electrocatalytic activity and coordination geometry at the Mn-center enforced by functionalized PDI ligands are underway in our laboratories.

EXPERIMENTAL PROCEDURES AND COMPUTATIONAL DETAILS

General Considerations. Unless stated otherwise, all synthetic manipulations were performed within an MBraun glovebox under an atmosphere of purified nitrogen. Anhydrous solvents were purified using a Pure Process Technology solvent system and stored in the glovebox over activated 4 Å molecular sieves and sodium before use.

DOI: 10.1021/acs.inorgchem.5b00315
Inorg. Chem. 2015, 54, 4475−4482

Benzene-d_6 was purchased from Cambridge Isotope Laboratories, and acetone-d_6 was purchased from Acros Organics and dried over 4 Å molecular sieves before use. Precursors $(CO)_5MnBr$ and 3-(diphenylphosphino)-1-propylamine were used as received from Strem Chemicals. Acetonitrile was purchased from Sigma-Aldrich and dried over calcium hydride and 4 Å molecular sieves before use. Tetrabutylammonium hexafluorophosphate was purchased from Sigma-Aldrich and used as received. Ferrocene was purchased from Acros Organics, while anhydrous MeOH was purchased from Sigma-Aldrich and dried over 4 Å molecular sieves before use. ^{Ph2PPr}PDI was prepared according to the published procedure.[30]

Solution ^{1}H nuclear magnetic resonance (NMR) spectra were recorded at room temperature on a Varian 400-MR 400 MHz NMR spectrometer. All ^{1}H and ^{13}C NMR chemical shifts (ppm) are reported relative to $Si(CH_3)_4$ using ^{1}H (residual) and ^{13}C chemical shifts of the solvent as secondary standards. ^{31}P NMR data are reported relative to H_3PO_4. UV−vis measurements were conducted using a Hitachi U-2010 spectrophotometer in quartz cuvettes with a path length of 1 cm. Infrared spectroscopy was performed using KBr pellets on a Bruker VERTEX 70 spectrophotometer with an MCT detector. Elemental analyses were performed at Robertson Microlit Laboratories Inc. (Ledgewood, NJ). Solution state magnetic susceptibility was determined via the Evans method.

X-ray Crystallography. Single crystals suitable for X-ray diffraction were coated with polyisobutylene oil in the glovebox and transferred to glass fiber with Apiezon N grease before mounting on the goniometer head of a Bruker APEX Diffractometer (Arizona State University) equipped with Mo Kα radiation. A hemisphere routine was used for data collection and determination of the lattice constants. The space group was identified, and the data were processed using the Bruker SAINT+ program and corrected for absorption using SADABS. The structures were solved using direct methods (SHELXS) completed by subsequent Fourier synthesis and refined by full-matrix, least-squares procedures on $[F^2]$ (SHELXS). The unit cell determined for **1** was found to possess two individual molecular units (see Tables S1 and S2 of the Supporting Information for additional crystallographic data).

Preparation of [(^{Ph2PPr}PDI)Mn(CO)][Br] (1). A 100 mL thick walled glass tube was charged with 0.150 g (0.245 mmol) of ^{Ph2PPr}PDI in 5 mL of THF. A 5 mL THF solution of 0.067 g (0.245 mmol) $(CO)_5MnBr$ was added to the tube. The clear orange solution was sealed under nitrogen and heated at 65 °C for 24 h while stirring. After 24 h, the reaction mixture was purple with a large amount of insoluble purple material in suspension. The headspace of the flask was evacuated on a Schlenk line using two freeze−pump−thaw cycles. The mixture was filtered through Celite, and the Celite pad was washed with 1 mL of THF to remove byproducts. Then, it was washed with 20 mL of acetone to obtain a deep purple filtrate, which was dried under vacuum. The resulting purple solid was washed twice with 2 mL portions of diethyl ether and further dried under vacuum. Recrystallization from acetonitrile at −35 °C afforded 0.0489 g (0.0629 mmol, 26% yield) of purple crystals identified as **1**. Elemental analysis for $C_{40}H_{41}N_3P_2MnOBr$: calcd C, 61.87%; H, 5.32%; N, 5.41%. Found: C, 62.01%; H, 5.40%; N, 5.53%. ^{1}H NMR (acetonitrile-d_3): δ (ppm) = 7.49 (m, 4H, *phenyl*), 7.39 (m, 6H, *phenyl*), 7.25 (m, 1H, *Py*), 7.14 (m, 2H, *Py*), 6.96 (m, 6H, *phenyl*), 6.48 (m, 4H, *phenyl*), 4.42 (m, 2H, CH_2), 3.91 (m, 2H, CH_2), 2.71 (m, 2H, CH_2), 2.58 (m, 4H, CH_2), 2.27 (m, 6H, CH_3), 1.96 (m, 2H, CH_2). ^{13}C NMR (acetonitrile-d_3): δ (ppm) = 165.1 (t, 2.3 Hz, *CO*), 157.4 (*imine C*), 137.3 (*phenyl*), 137.0 (*phenyl*), 132.8 (*phenyl*), 132.6 (*phenyl*), 132.5 (*phenyl*), 131.6 (*phenyl*), 131.3 (*phenyl*), 130.3 (*phenyl*), 129.7 (*phenyl*), 129.3 (*phenyl*), 58.9 (NCH_2), 28.6 (CH_3), 24.6 (m, PCH_2), 15.3 (CH_2). ^{31}P{^{1}H} NMR (acetonitrile-d_3): δ (ppm) = 55.42 (s, PPh_2). IR (KBr): ν_{CO} = 1825 cm^{-1}. UV−vis (from 9 independent concentrations in acetonitrile): λ_{max} = 368 nm (ε = 4050 M^{-1}cm^{-1}), 528 nm (ε = 6840 M^{-1}cm^{-1}), 672 nm (ε = 830 M^{-1}cm^{-1}).

Preparation of (^{Ph2PPr}PDI)MnBr (2). A thick walled glass tube was charged with 0.151 g (0.247 mmol) of ^{Ph2PPr}PDI in approximately 4 mL of THF. A 10 mL THF solution of 0.068 g (0.247 mmol) $(CO)_5MnBr$ was added, and the tube was sealed under N_2 atmosphere. The resulting orange solution was stirred at 80 °C for 72 h. An intense blue solution, with a small amount of insoluble purple material had formed. The headspace of the flask was evacuated on a Schlenk line using two freeze−pump−thaw cycles to remove carbon monoxide. The blue solution was vacuum filtered through Celite, and THF was removed *in vacuo* to obtain a deep blue solid. This solid was washed three times with 4 mL portions of pentane and further dried to afford 0.140 g (0.187 mmol, 76% yield) of **2**. Elemental analysis for $C_{39}H_{41}N_3P_2MnBr$: calcd C, 62.58%; H, 5.52%; N, 5.61%. Found: C, 62.37%; H, 5.81%; N, 5.38%. Magnetic Susceptibility: μ_{eff} = 4.4 μ_B (benzene-d_6, 25 °C). ^{1}H NMR (benzene-d_6, 25 °C): δ (ppm) = 74.68 (peak width at 1/2 height = 4224 Hz). ^{13}C NMR (benzene-d_6, 25 °C): no resonances located. UV−vis (from 9 independent concentrations in THF, Figure S16 (Supporting Information)): λ_{max} = 361 nm (ε = 3040 M^{-1}cm^{-1}), 614 nm (ε = 2650 M^{-1} cm^{-1}).

Cyclic Voltammetry. All experiments were conducted using a three-electrode system with a glassy carbon working electrode (3 mm diameter with a surface area of 0.0707 cm^2), a silver wire pseudoreference electrode, and a platinum counter electrode. The working electrode was cleaned with diamond paste (0.1 μm Glennel UB Formulation, from Electron Microscopy Sciences) and washed with water and acetonitrile (MeCN) before use. The reference electrode was dipped into 1 M HCl and air-dried prior to use. All voltammograms are reported relative to ferrocene, which was used as an internal standard. Buffer solutions were prepared by dissolving 15 mM of each MES, TAPS, HEPES, and CHES in water. Pseudo-pH values were measured using an ACUMET BASIC AB15 (Fisher Scientific) pH-meter using an AcuTupH (13−620−183A) electrode. Each measurement was taken on 5 mL of analyte solution.

Bulk Electrolysis. Bulk electrolysis experiments were undertaken in a sealed BASi bulk electrolysis cell prepared in a glovebox, and gas chromatography was used to quantify the H_2 and CO produced. The working electrode was a reticulated vitreous carbon electrode (cylinder of 40 mm diameter, 50 mm height, and 5 mm depth). A nonaqueous (MeCN) Ag/AgCl reference electrode was placed in a separate compartment and connected via a fine porosity glass frit. A platinum wire was used as counter electrode. A 50 mL soluton of 5 mM **1** in 0.1 M $[NBu_4][PF_6]$/MeCN was used with 1.05 M MeOH and saturated with CO_2. The cell had a head space of 38.75 mL. Gas withdrawals from the headspace were made with a Hamilton 1750 SL locking gastight syringe and were compensated with an equal addition of argon. Following calibration with known concentrations of H_2 and CO over the region 0−3.0% (volume %), a Varian CP-3800 gas chromatograph (thermal conductivity detector, Alltech Porapak Q 80/100 column, Argon as carrier gas) was used to determine the concentrations of CO and H_2 in the headspace. The CO concentration remained below detection limits. The Faradaic efficiency for the electrolytic production of H_2 was 96.7% with a TOF of 0.176 h^{-1}.

Computational Details. Calculations were carried out using DFT as implemented in the Jaguar 8.1 suite of ab initio quantum chemistry programs.[34] Geometry optimizations were performed with the PBE functional[35] using the 6-31G** basis set.[36] Mn was represented using the Los Alamos LACVP basis that includes relativistic effective core potentials.[37] The energies of the optimized structures were reevaluated by additional single point calculations on each optimized geometry using Dunning's correlation consistent triple-ζ basis set cc-pVTZ(-f) that includes a double set of polarization functions.[38] For Mn, we used a modified version of LACVP, designated as LACV3P, in which the exponents were decontracted to match the effective core potential with triple-ζ quality. As mentioned in the text, we also performed single point energy calculations using the B3LYP functional as well.[39−43] Vibrational/rotational/translational entropies were included using standard thermodynamic approximations. Solvation energies were evaluated by a self-consistent reaction field (SCRF) approach based on accurate numerical solutions of the linearized Poisson−Boltzmann equation.[44−47] Solvation calculations were carried out at the optimized gas phase geometry employing the dielectric constant of ε = 37.5 (acetonitrile). As is the case for all continuum models, the solvation energies are subject to empirical parametrization of the atomic radii that are used to generate the solute surface. We employ the standard

DOI: 10.1021/acs.inorgchem.5b00315
Inorg. Chem. 2015, 54, 4475−4482

set of optimized radii for H (1.150 Å), C (1.900 Å), N (1.600 Å), O (1.600 Å), P (2.074 Å), and Mn (1.480 Å). Convergence to plausible electronic states that correspond to conceptually meaningful electronic configurations was monitored by carefully observing the Mulliken spin densities and visualizing the frontier molecular orbitals. AF singlet states were modeled using Noodleman's broken symmetry (BS) formalism without spin projection.[48−50] Energy components have been computed as follows following the protocol of our previous work. The change in solution phase free energy $\Delta G(\mathrm{sol})$ was calculated as follows:

$$\Delta G(\mathrm{sol}) = \Delta G(\mathrm{gas}) + \Delta\Delta G_{\mathrm{solv}}$$

$$\Delta G(\mathrm{gas}) = \Delta H(\mathrm{gas}) - T\Delta S(\mathrm{gas})$$

$$\Delta H(\mathrm{gas}) = \Delta E(\mathrm{SCF}) + \Delta ZPE$$

$\Delta G(\mathrm{gas})$ = change in gas phase free energy; $\Delta\Delta G_{\mathrm{solv}}$ = change in free energy of solvation; $\Delta H(\mathrm{gas})$ = change in gas phase enthalpy; T = temperature (298.15 K); $\Delta S(\mathrm{gas})$ = change in gas phase entropy; $\Delta E(\mathrm{SCF})$ = self-consistent field energy, i.e., "raw" electronic energy as calculated at the triple-ζ level; ΔZPE = change in vibrational zero point energy. All structures were determined to be minima with no imaginary frequencies.

■ ASSOCIATED CONTENT

Supporting Information

Crystallographic information for **1** (CCDC-1044759), optimized coordinates, vibrational frequencies, and energetics from DFT analysis, and multinuclear NMR spectroscopic and cyclic voltammograms. This material is available free of charge via the Internet at http://pubs.acs.org.

■ AUTHOR INFORMATION

Corresponding Authors

*(M.-H.B.) Phone: 812-856-0454. E-mail: mbaik@indiana.edu.
*(A.K.J.) Phone: 480-965-0356. E-mail: anne.katherine.jones@asu.edu.
*(R.J.T.) Phone: 480-727-8930. E-mail: ryan.trovitch@asu.edu.

Notes

The authors declare no competing financial interest.

■ ACKNOWLEDGMENTS

We thank the Research Corporation for Science Advancement for a Scialog Collaborative Innovation Award (M.-H.B. and R.J.T) and a Scialog Award (M.-H. B). Partial support was provided by the Center for Bioinspired Solar Fuel Production, an Energy Frontier Research Center funded by the U.S. Department of Energy, Office of Basic Energy Sciences under Award Number DE-SC0001016. M.-H.B. thanks the National Science Foundation (0116050, CHE-0645381, and CHE-1001589) for support. A.K.J. thanks the Institut D'Etudes Avancées Exploratoire Méditerranéen de l'Interdisciplinarité for support.

■ REFERENCES

(1) Walter, M. G.; Warren, E. L.; McKone, J. R.; Boettcher, S. W.; Mi, Q.; Santori, E. A.; Lewis, N. S. *Chem. Rev.* **2010**, *110*, 6446−6473.

(2) (a) Gust, D.; Moore, T. A.; Moore, A. L. *Acc. Chem. Res.* **2009**, *42*, 1890−1898. (b) Gust, D.; Moore, T. A.; Moore, A. L. *Acc. Chem. Res.* **2001**, *34*, 40−48. (c) Gust, D.; Moore, T. A.; Moore, A. L. *Acc. Chem. Res.* **1993**, *26*, 198−205.

(3) Nocera, D. G. *Acc. Chem. Res.* **2012**, *45*, 767−776.

(4) For representative Fe catalysts see: (a) Roy, S.; Mazinani, S. K. S.; Groy, T. L.; Gan, L.; Tarakeshwar, P.; Mujica, V.; Jones, A. K. *Inorg. Chem.* **2014**, *53*, 8919−8929. (b) Darmon, J. M.; Raugei, S.; Liu, T.; Hulley, E. B.; Weiss, C. J.; Bullock, R. M.; Helm, M. L. *ACS Catal.* **2014**, *4*, 1246−1260. (c) Gloaguen, F.; Rauchfuss, T. B. *Chem. Soc. Rev.* **2009**, *38*, 100−108.

(5) For representative Co catalysts see: (a) McCrory, C. C. L.; Uyeda, C.; Peters, J. C. *J. Am. Chem. Soc.* **2012**, *134*, 3164−3170. (b) Dempsey, J. L.; Brunschwig, B. S.; Winkler, J. R.; Gray, H. B. *Acc. Chem. Res.* **2009**, *42*, 1995−2004. (c) Jacques, P.-A.; Artero, V.; Pécaut, J.; Fontecave, M. *Proc. Natl. Acad. Sci. U.S.A.* **2009**, *106*, 20627−20632. (d) Hu, X.; Brunschwig, B. S.; Peters, J. C. *J. Am. Chem. Soc.* **2007**, *129*, 8988−8998. (e) Artero, V.; Fontecave, M. *Coord. Chem. Rev.* **2005**, *249*, 1518−1535.

(6) For representative Ni catalysts see: (a) Gan, L.; Groy, T. L.; Tarakeshwar, P.; Mazinani, S. K. S.; Shearer, J.; Mujica, V.; Jones, A. K. *J. Am. Chem. Soc.* **2015**, *137*, 1109−1115. (b) Helm, M. L.; Stewart, M. P.; Bullock, R. M.; DuBois, M. R.; DuBois, D. L. *Science* **2011**, *333*, 863−866. (c) Kilgore, U. J.; Roberts, J. A. S.; Pool, D. H.; Appel, A. M.; Stewart, M. P.; DuBois, M. R.; Dougherty, W. G.; Kassel, W. S.; Bullock, R. M.; DuBois, D. L. *J. Am. Chem. Soc.* **2011**, *133*, 5861−5872. (d) Wilson, A. D.; Shoemaker, R. K.; Miedaner, A.; Muckerman, J. T.; DuBois, D. L.; DuBois, M. R. *Proc. Natl. Acad. Sci. U.S.A.* **2007**, *104*, 6951−6956. (e) Wilson, A. D.; Newell, R. H.; McNevin, M. J.; Muckerman, J. T.; DuBois, M. R.; DuBois, D. L. *J. Am. Chem. Soc.* **2006**, *128*, 358−366.

(7) Lewis, N. S.; Nocera, D. G. *Proc. Natl. Acad. Sci. U.S.A.* **2006**, *103*, 15729−15735.

(8) Crabtree, G. W.; Dresselhaus, M. S.; Buchanan, M. V. *Phys. Today* **2004**, *57*, 39−44.

(9) (a) Benson, E. E.; Kubiak, C. P.; Sathrum, A. J.; Smieja, J. M. *Chem. Soc. Rev.* **2009**, *38*, 89−99. (b) Kumar, B.; Llorente, M.; Froehlich, J.; Dang, T.; Sathrum, A.; Kubiak, C. P. *Annu. Rev. Phys. Chem.* **2012**, *63*, 541−69.

(10) (a) Schneider, J.; Jia, H.; Muckerman, J. T.; Fujita, E. *Chem. Soc. Rev.* **2012**, *41*, 2036−2051. (b) Doherty, M. D.; Grills, D. C.; Muckerman, J. T.; Polyansky, D. E.; Fujita, E. *Coord. Chem. Rev.* **2010**, *254*, 2472−2482. (c) Fujita, E. *Coord. Chem. Rev.* **1999**, *185*−*186*, 373−384.

(11) For Fe catalysts see: (a) Costentin, C.; Passard, G.; Robert, M.; Savéant, J.-M. *Proc. Natl. Acad. Sci. U.S.A.* **2014**, *111*, 14990−14994. (b) Costentin, C.; Passard, G.; Robert, M.; Savéant, J.-M. *J. Am. Chem. Soc.* **2014**, *136*, 11821−11829. (c) Costentin, C.; Drouet, S.; Robert, M.; Savéant, J.-M. *Science* **2012**, *338*, 90−94. (d) Thammavongsy, Z.; Seda, T.; Zakharov, L. N.; Kaminsky, W.; Gilbertson, J. D. *Inorg. Chem.* **2012**, *51*, 9168−9170. (e) Chen, J.; Szalda, D. J.; Fujita, E.; Creutz, C. *Inorg. Chem.* **2010**, *49*, 9380−9391. (f) Grodkowski, J.; Neta, P. *J. Phys. Chem. A* **2000**, *104*, 4475−4479. (g) Dhanasekaran, T.; Grodkowski, J.; Neta, P.; Hambright, P.; Fujita, E. *J. Phys. Chem. A* **1999**, *103*, 7742−7748. (h) Grodkowski, J.; Behar, D.; Neta, P.; Hambright, P. *J. Phys. Chem. A* **1997**, *101*, 248−254. (i) Bhugun, I.; Lexa, D.; Savéant, J.-M. *J. Am. Chem. Soc.* **1996**, *118*, 1769−1776. (j) Bhugun, I.; Lexa, D.; Savéant, J.-M. *J. Am. Chem. Soc.* **1994**, *116*, 5015−5016. (k) Hammouche, M.; Lexa, D.; Momenteau, M.; Savéant, J.-M. *J. Am. Chem. Soc.* **1991**, *113*, 8455−8466. (l) Hammouche, M.; Lexa, D.; Savéant, J.-M. *J. Electroanal. Chem.* **1988**, *249*, 347−351.

(12) For Co catalysts see: (a) Ogata, T.; Yamamoto, Y.; Wada, Y.; Murakoshi, K.; Kusaba, M.; Nakashima, N.; Ishida, A.; Takamuku, S.; Yanagida, S. *J. Phys. Chem.* **1995**, *99*, 11916−11922. (b) Ogata, T.; Yanagida, S.; Brunschwig, B. S.; Fujita, E. *Energy Convers. Manage.* **1995**, *36*, 669−672. (c) Matsuoka, S.; Yamamoto, K.; Ogata, T.; Kusaba, M.; Nakashima, N.; Fujita, E.; Yanagida, S. *J. Am. Chem. Soc.* **1993**, *115*, 601−609. (d) Fujita, E.; Szalda, D. J.; Creutz, C.; Sutin, N. *J. Am. Chem. Soc.* **1988**, *110*, 4870−4871. (e) Fisher, B.; Eisenberg, R. *J. Am. Chem. Soc.* **1980**, *102*, 7361−7363.

(13) For Ni catalysts see: (a) Thoi, V. S.; Chang, C. J. *Chem. Commun.* **2011**, *47*, 6578−6580. (b) Simón-Manso, E.; Kubiak, C. P. *Organometallics* **2005**, *24*, 96−102. (c) Fujita, E.; Brunschwig, B. S.; Ogata, T.; Yanagida, S. *Coord. Chem. Rev.* **1994**, *132*, 195−200. (d) Craig, C. A.; Spreer, L. O.; Otvos, J. W.; Calvin, M. *J. Phys. Chem.* **1990**, *94*, 7957−7960. (e) Daniele, S.; Ugo, P.; Bontempelli, G.; Fiorani, M. *J. Electroanal. Chem.* **1987**, *219*, 259−271. (f) Beley, M.;

DOI: 10.1021/acs.inorgchem.5b00315
Inorg. Chem. 2015, 54, 4475−4482

Collin, J.-P.; Ruppert, R.; Sauvage, J.-P. *J. Am. Chem. Soc.* **1986**, *108*, 7461−7467. (g) Meshitsuka, S.; Ichikawa, M.; Tamaru, K. *J. Chem. Soc., Chem. Commun.* **1974**, 158−159.
(14) Bourrez, M.; Molton, F.; Chardon-Noblat, S.; Deronzier, A. *Angew. Chem., Int. Ed.* **2011**, *50*, 9903−9906.
(15) (a) Smieja, J. M.; Benson, E. E.; Kumar, B.; Grice, K. A.; Seu, C. S.; Miller, A. J. M.; Mayer, J. M.; Kubiak, C. P. *Proc. Natl. Acad. Sci. U.S.A.* **2012**, *109*, 15646−15650. (b) Smieja, J. M.; Kubiak, C. P. *Inorg. Chem.* **2010**, *49*, 9283−9289. (c) Kumar, B.; Smieja, J. M.; Kubiak, C. P. *J. Phys. Chem. C* **2010**, *114*, 14220−14223. (d) Johnson, F. P. A.; George, M. W.; Hartl, F.; Turner, J. J. *Organometallics* **1996**, *15*, 3374−3387. (e) Sullivan, B. P.; Bolinger, C. M.; Conrad, D.; Vining, W. J.; Meyer, T. J. *J. Chem. Soc., Chem. Commun.* **1985**, 1414−1416. (f) Hawecker, J.; Lehn, J.-M.; Ziessel, R. *J. Chem. Soc., Chem. Commun.* **1984**, 328−330.
(16) Smieja, J. M.; Sampson, M. D.; Grice, K. A.; Benson, E. E.; Froehlich, J. D.; Kubiak, C. P. *Inorg. Chem.* **2013**, *52*, 2484−2491.
(17) Sampson, M. D.; Nguyen, A. D.; Grice, K. A.; Moore, C. E.; Rheingold, A. L.; Kubiak, C. P. *J. Am. Chem. Soc.* **2014**, *136*, 5460−5471.
(18) Takeda, H.; Koizumi, H.; Okamoto, K.; Ishitani, O. *Chem. Commun.* **2014**, *50*, 1491−1493.
(19) Walsh, J. J.; Neri, G.; Smith, C. L.; Cowan, A. J. *Chem. Commun.* **2014**, *50*, 12698−12701.
(20) For an example of Mn-catalyzed proton reduction see: Valyaev, D. A.; Peterleitner, M. G.; Semeikin, O. V.; Utegenov, K. I.; Ustynyuk, N. A.; Sournia-Saquet, A.; Lugan, N.; Lavigne, G. *J. Organomet. Chem.* **2007**, *692*, 3207−3211.
(21) For recent contributions see: (a) Riplinger, C.; Sampson, M. D.; Ritzmann, A. M.; Kubiak, C. P. *J. Am. Chem. Soc.* **2014**, *136*, 16285−16298. (b) Bourrez, M.; Orio, M.; Molton, F.; Vezin, H.; Duboc, C.; Deronzier, A.; Chardon-Noblat, S. *Angew. Chem., Int. Ed.* **2014**, *53*, 240−243. (c) Grills, D. C.; Farrington, J. A.; Layne, B. H.; Lymar, S. V.; Mello, B. A.; Preses, J. M.; Wishart, J. F. *J. Am. Chem. Soc.* **2014**, *136*, 5563−5566.
(22) (a) Zeng, Q.; Tory, J.; Hartl, F. *Organometallics* **2014**, *33*, 5002−5008. (b) Vollmer, M. V.; Machan, C. W.; Clark, M. L.; Antholine, W. E.; Agarwal, J.; Schaefer, H. F., III; Kubiak, C. P.; Walensky, J. R. *Organometallics* **2015**, *34*, 3−12.
(23) (a) Agarwal, J.; Stanton, C. J., III; Shaw, T. W.; Vandezande, J. E.; Majetich, G. F.; Bocarsly, A. B.; Schaefer, H. F., III *Dalton Trans.* **2015**, *44*, 2122−2131. (b) Agarwal, J.; Shaw, T. W.; Stanton, C. J., III; Majetich, G. F.; Bocarsly, A. B.; Schaefer, H. F., III *Angew. Chem., Int. Ed.* **2014**, *53*, 5152−5155.
(24) (a) Mukhopadhyay, T. K.; Feller, R. K.; Rein, F. N.; Henson, N. J.; Smythe, N. C.; Trovitch, R. J.; Gordon, J. C. *Chem. Commun.* **2012**, *48*, 8670−8672. (b) Scarborough, C. C.; Wieghardt, K. *Inorg. Chem.* **2011**, *50*, 9773−9793. and references therein. (c) Irwin, M.; Jenkins, R. K.; Denning, M. S.; Krämer, T.; Grandjean, F.; Long, G. J.; Herchel, R.; McGrady, J. E.; Goicoechea, J. M. *Inorg. Chem.* **2010**, *49*, 6160−6171. (d) Kraft, S. J.; Fanwick, P. E.; Bart, S. C. *Inorg. Chem.* **2010**, *49*, 1103−1110. (e) Roitershtein, D.; Domingos, Ã.; Pereira, L. C. J.; Ascenso, J. R.; Marques, N. *Inorg. Chem.* **2003**, *42*, 7666−7673. (f) Schultz, M.; Boncella, J. M.; Berg, D. J.; Tilley, T. D.; Anderson, R. A. *Organometallics* **2001**, *21*, 460−472. (g) Evans, W. J.; Drummond, D. K. *J. Am. Chem. Soc.* **1989**, *111*, 3329−3335.
(25) (a) Porter, T. M.; Hall, G. B.; Groy, T. L.; Trovitch, R. J. *Dalton Trans.* **2013**, *42*, 14689−14692. (b) Khusniyarov, M. M.; Weyhermüller, T.; Bill, E.; Wieghardt, K. *J. Am. Chem. Soc.* **2009**, *131*, 1208−1221. and references therein. (c) Muresan, N.; Lu, C. C.; Ghosh, M.; Peters, J. C.; Abe, M.; Henling, L. M.; Weyhermöller; Bill, E.; Wieghardt, K. *Inorg. Chem.* **2008**, *47*, 4579−4590. (d) Muresan, N.; Chlopek, K.; Weyhermüller, T.; Neese, F.; Wieghardt, K. *Inorg. Chem.* **2007**, *46*, 5327−5337. (e) Khusniyarov, M. M.; Harms, K.; Burghaus, O.; Sundermeyer, J. *Eur. J. Inorg. Chem.* **2006**, 2985−2996.
(26) (a) Bart, S. C.; Chlopek, K.; Bill, E.; Bouwkamp, M. W.; Lobkovsky, E.; Neese, F.; Wieghardt, K.; Chirik, P. J. *J. Am. Chem. Soc.* **2006**, *128*, 13901−13912. (b) Knijnenburg, Q.; Gambarotta, S.; Budzelaar, P. H. M. *Dalton Trans.* **2006**, 5442−5448. (c) de Bruin, B.; Bill, E.; Bothe, E.; Weyhermüller, T.; Wieghardt, K. *Inorg. Chem.* **2000**, *39*, 2936−2947.
(27) Mukhopadhyay, T. K.; Flores, M.; Groy, T. L.; Trovitch, R. J. *J. Am. Chem. Soc.* **2014**, *136*, 882−885.
(28) Cavanaugh, M. D.; Gregg, B. T.; Cutler, A. R. *Organometallics* **1996**, *15*, 2764−2769.
(29) Trovitch, R. J. *Synlett* **2014**, *25*, 1638−1642.
(30) Ben-Daat, H.; Hall, G. B.; Groy, T. L.; Trovitch, R. J. *Eur. J. Inorg. Chem.* **2013**, 4430−4442.
(31) Russell, S. K.; Bowman, A. C.; Lobkovsky, E.; Wieghardt, K.; Chirik, P. J. *Eur. J. Inorg. Chem.* **2012**, 535−545.
(32) Gennaro, A.; Isse, A. A.; Vianello, E. *J. Electroanal. Chem.* **1990**, *289*, 203−215.
(33) Hydrosilylation reactions using (^{Ph2PPr}PDI)Mo(CO) have recently been found to proceed following phosphine donor dissociation. Please see: Pal, R.; Groy, T. L.; Bowman, A. C.; Trovitch, R. J. *Inorg. Chem.* **2014**, *53*, 9357−9365.
(34) *Jaguar*, version 8.1; Schrodinger, LLC: New York, NY, 2013.
(35) (a) Perdew, J. P.; Burke, K.; Ernzerhof, M. *Phys. Rev. Lett.* **1996**, *77*, 3865−3868. (b) Perdew, J. P.; Burke, K.; Ernzerhof, M. *Phys. Rev. Lett.* **1997**, *78*, 1396.
(36) Rassolov, V.; Pople, J. A.; Ratner, M.; Windus, T. L. *J. Chem. Phys.* **1998**, *109*, 1223−1229.
(37) (a) Hay, P. J.; Wadt, W. R. *J. Chem. Phys.* **1985**, *82*, 270−283. (b) Wadt, W. R.; Hay, P. J. *J. Chem. Phys.* **1985**, *82*, 284−298.
(38) Dunning, T. H., Jr. *J. Chem. Phys.* **1989**, *90*, 1007−1023.
(39) Becke, A. D. *Phys. Rev. A* **1988**, *38*, 3098−3100.
(40) Becke, A. D. *J. Chem. Phys.* **1993**, *98*, 5648−5652.
(41) Vosko, S. H.; Wilk, L.; Nusair, M. *Can. J. Phys.* **1980**, *58*, 1200−1211.
(42) Lee, C.; Yang, W.; Parr, R. G. *Phys. Rev. B* **1988**, *37*, 785−789.
(43) Stephens, P. J.; Devlin, F. J.; Chabalowski, C. F.; Frisch, M. J. *J. Phys. Chem.* **1994**, *98*, 11623−11627.
(44) Marten, B.; Kim, K.; Cortis, C.; Friesner, R. A.; Murphy, R. B.; Ringnalda, M. N.; Sitkoff, D.; Honig, B. *J. Phys. Chem.* **1996**, *100*, 11775−11788.
(45) Friedrichs, M.; Zhou, R. H.; Edinger, S. R.; Friesner, R. A. *J. Phys. Chem. B* **1999**, *103*, 3057−3061.
(46) Edinger, S. R.; Cortis, C.; Shenkin, P. S.; Friesner, R. A. *J. Phys. Chem. B* **1997**, *101*, 1190−1197.
(47) Rashin, A. A.; Honig, B. *J. Phys. Chem.* **1985**, *89*, 5588−5593.
(48) Noodleman, L. *J. Chem. Phys.* **1981**, *74*, 5737−5743.
(49) Noodleman, L.; Lovell, T.; Han, W.-G.; Li, J.; Himo, F. *Chem. Rev.* **2004**, *104*, 459−508.
(50) Noodleman, L.; Davidson, E. R. *Chem. Phys.* **1986**, *109*, 131−143.

DOI: 10.1021/acs.inorgchem.5b00315
Inorg. Chem. 2015, 54, 4475−4482